



Oxide Formation at the Sulfide Film-Copper Interface in Anoxic Sulfide Solution and On-Line Sulfide Detection Via Linear Polarization Resistance

Kai Arstila¹ | Erik Bergendal² D | Ahsan Chonche¹ D | Tiina Ikäläinen¹ | Christina Lilja² D | Zaiqing Que¹ | Timo Saario¹

¹VTT Technical Research Centre of Finland Ltd, Espoo, Finland | ²Swedish Nuclear Fuel and Waste Management Company, SKB, Solna, Sweden

Correspondence: Ahsan Chonche (ahsan.chonche@vtt.fi)

Received: 15 August 2025 | Revised: 26 September 2025 | Accepted: 1 October 2025

Funding: The study was supported by the SKB, the Swedish Nuclear Fuel and Waste Management Co. (Solna, Sweden).

Keywords: copper | copper oxide | linear polarization resistance (LPR) | metallographic preparation | sulfide

ABSTRACT

The observation of a thin oxide film on oxygen free phosphorous doped copper after several days of exposure in supposedly anoxic conditions poses several questions, where the most straight-forward answers regarding sample preparation and handling is oftentimes overlooked. In an effort to minimize the environmental factors contributing to the oxide formation on the copper surface, a flow through cell arrangement was built to investigate the oxide formation at the Cu–Cu₂S interface after exposure to anoxic sulfide containing phosphate buffer solution. The post exposure characterization by scanning electron microscopy and focused ion beam revealed no oxide formation on the copper surface in the absence of oxygen, while the exposure of the copper surface during the metallographic sample preparation phase, which employs the use of aerated water, causes the formation of copper oxide. Furthermore, a novel technique for noninvasive, semi-quantitative, and on-line sulfide determination is presented. The anodic current density determined from the linear polarization resistance of copper in sulfide solution was found to linearly increase with sulfide concentration.

1 | Introduction

The Swedish Nuclear Fuel and Waste Management Co (SKB) and the Finnish final waste disposal company Posiva Oy have chosen oxygen free phosphorous doped copper (Cu-OFP) as corrosion barrier material for disposal of spent nuclear fuel. The canisters are to be deposited at a depth of roughly –450 m in the bedrock, surrounded by bentonite clay [1–3]. Extensive studies have been conducted to understand the corrosion mechanism and behavior of the corrosion film formed on Cu-OFP under simulated conditions expected in the bedrock for short- and long-term exposures [4–8]. Particularly, for tests performed in anoxic sulfide solutions, sometimes the presence of oxygen is found in the surface films, implying a coexistence of Cu₂O and Cu₂S [9–11]. Several reasons for the formation of this oxide can be found in

scientific literature. First, presence of a pre-existing thin oxide layer on polished Cu samples, which can occur due to exposure to air. When exposed to the sulfide solution such a thin oxide layer is expected to be transformed to Cu₂S. Second, in the case when sulfide exposure tests are performed on a pre-oxidized Cu surface, some remnants of this oxide layer are expected [12, 13]. Additionally, in presence of chlorides along with sulfides in borate-buffered test solution, the oxide can form through direct oxidation of the Cu surface or through hydrolysis of the adsorbed CuCl layer and by dissolution of the complex copper chloride ions. On the other hand, studies such as [7, 14] have shown no role of Cu₂O formation on Cu-OFP in chloride and sulfate containing sulfide solutions, because thermodynamically Cu₂S is more stable than Cu₂O in sulfide solutions. In an effort to clarify the formation and presence of an oxide film in a sulfide solution, the

This is an open access article under the terms of the Creative Commons Attribution License, which permits use, distribution and reproduction in any medium, provided the original work is properly cited.

© 2025 The Author(s). Materials and Corrosion published by Wiley-VCH GmbH.

present study was conducted, to investigate whether an oxide film can form and exist at the Cu-Cu₂S interface in an anoxic, sulfidecontaining, phosphate-buffered solution without chlorides. The tests were performed using a flow-through cell arrangement for careful atmosphere control during exposure and sample handling post exposure. Additionally, the sulfide film formation on Cu is known to be largely influenced by the concentration and diffusion of the sulfide in the solution [13, 15]. In this regard, and especially at low concentrations, it is of great interest to be able to determine the sulfide concentration in the test solution or the groundwater, by on-line measurements with minimal solution disturbance. There is already existing work demonstrating the Cu corrosion monitoring in bentonite clay by implementing a combination of methods such as electrochemical impedance spectroscopy and coupled multi-electrode array (CMEA) [16]. In the present work, however, a method for semi-quantitative, undisruptive, and on-line sulfide concentration determination is presented. Using anodic current densities from linear polarization resistance (LPR) of Cu-OFP, varying concentrations of HS is determined in sulfide solutions under static conditions.

2 | Experimental

2.1 | Sample and Buffer Solution Preparation

The Cu used in the study is of type Cu-OFE with the addition of 30–100 wt-ppm phosphorous for increased creep ductility. The average phosphorous and impurity composition of the Cu-OFP (99.992% Cu) [17] is provided in Table 1. Four samples of Cu-OFP measuring $20 \times 20 \times 3$ mm provided by SKB were cut and prepared with a final polishing made by P1200 grade SiC paper before exposure in the flow-through cell arrangement. The working electrode samples for LPR measured $15 \times 20 \times 1$ mm and were also polished to P1200 grade SiC.

Phosphate buffer solution (pH = 7.2) with 10^{-3} M sulfide was used in the experiments. The phosphorous buffer solution was prepared using Na₂HPO₄'2H₂O and NaH₂PO₄'2H₂O supplied by VWR Chemicals BDH*. The prepared buffer was stored in an airtight glass feed bottle and bubbled with 99.999% N₂ gas for 24 h to remove oxygen. An amount of 2.0 g of sodium sulfide (Na₂S'6H₂O, produced by Acros Oragnics B.V.B.A, stored in refrigerated condition and used without recrystallization) was added to the buffer in the glass feed bottle to achieve the 32 mg/L (10^{-3} M) concentration and after which the feed bottle was additionally purged with the 99.999% N₂ gas for another 10 min to remove any air entering the bottle during addition of the sulfide crystals.

2.2 | Flow Through Cell Arrangement

A series arrangement of flow-through cells was built, schematically depicted in Figure 1. It consisted of two small

TABLE 1 | Average phosphorous and impurity concentration of the Cu-OFP, in wt-ppm [17].

Element	P	S	0	Н
wt-ppm	58.7	5.4	3	0.43

flow-through cells manufactured from AISI 316 stainless steel. The internal volume of each cell was 1 L. Preconditioning of the flowthrough cells was performed to saturate the cell walls and pipe with sulfide before exposing the samples. The cells were connected to supply lines, and buffer solution with 10^{-3} M (32 mg/L) sulfide was directed through them via a Cole-Parmer Instruments Co. peristaltic pump for about 48 h. After 48 h of preconditioning the flow-through cell arrangement, two samples were freely suspended inside each cell, supported by PTFE covered Ni wire so that the samples were in no contact with each other and the cell walls. The phosphate buffer solution (pH = 7.2) with 10^{-3} M sulfide was again pumped through the cells for 48 h. Initially, the flow rate was set to maximum until the cells were filled with the buffer solution after which the flow rate was adjusted to 3 mL/min for the 48-h test duration. A small volume of sulfide solution was collected in a vial at the outlet valve and the sulfide concentration was measured using CHEMetrics VACUettes Kit K-9510D (0-30 & 30-300 ppm), by AquaPhoenix Scientific in the beginning, after 24 h and at the end of the test and was found to be consistent at 10^{-3} M. The accuracy of the measuring method in experience is about $\pm 15\%$ at this concentration of 10^{-3} M.

At the end of the test, the two cells were isolated from each other with a valve. The sulfide solution in Cell 1 was emptied by passing N₂ gas. A continuous stream of N₂ gas flow was maintained through Cell 1 for the whole period before transferring the cell to the scanning electron microscopy/focused ion beam (SEM/FIB) chamber. Cell 1 was opened in the SEM/FIB-room after approximately 100 h since the solution was removed from the cell. During this period, the cell was continuously kept under a nitrogen blanket. The transfer of one of the samples from the cell to the SEM/FIB-chamber took about 4 min, during which the sample was briefly exposed to air. No cross-sectional preparation outside of the SEM/FIB-chamber was performed for the samples from Cell 1. Unlike Cell 1, Cell 2 was immediately opened once the sulfide solution had been emptied using N2 gas. Both the samples from Cell 2 were retrieved, rinsed with type 1 water (ionic conductivity of 18.3 M Ω ·cm) [18] followed by ethanol and gently dried with blowing air. The samples from Cell 2 were then prepared for normal cross-sectional study under SEM/FIB.

2.3 | Electrochemical Set Up

The electrochemical set up comprised of a Cu-OFP sample as working electrode, a platinum counter electrode, and a 0.5 M KCl/AgCl/Ag reference electrode. LPR measurements were performed at a sweep rate of 0.167 mV/s with an Ivium Compactstat equipped with a frequency-response analyzer and high sensitivity modules. This experiment was performed in an autoclave with continuous flow-through of the sulfide buffer solution. Initially, the sample was exposed to 10^{-3} M of sulfide containing buffer solution for about 48 h in the autoclave, after which the flow was switched to the same phosphate buffer feed without sulfide using a three-way connection in the feedwater line. At this point, the LPR measurement was initiated to run consecutively while simultaneously the sulfur concentration inside the autoclave was being depleted. It took approximately 3.5 h. to remove sulfide from the water completely. The depleting sulfide concentration was frequently measured using the CHEMetrics sulfide analyzing vacuum glass kit.

2 Materials and Corrosion, 2025

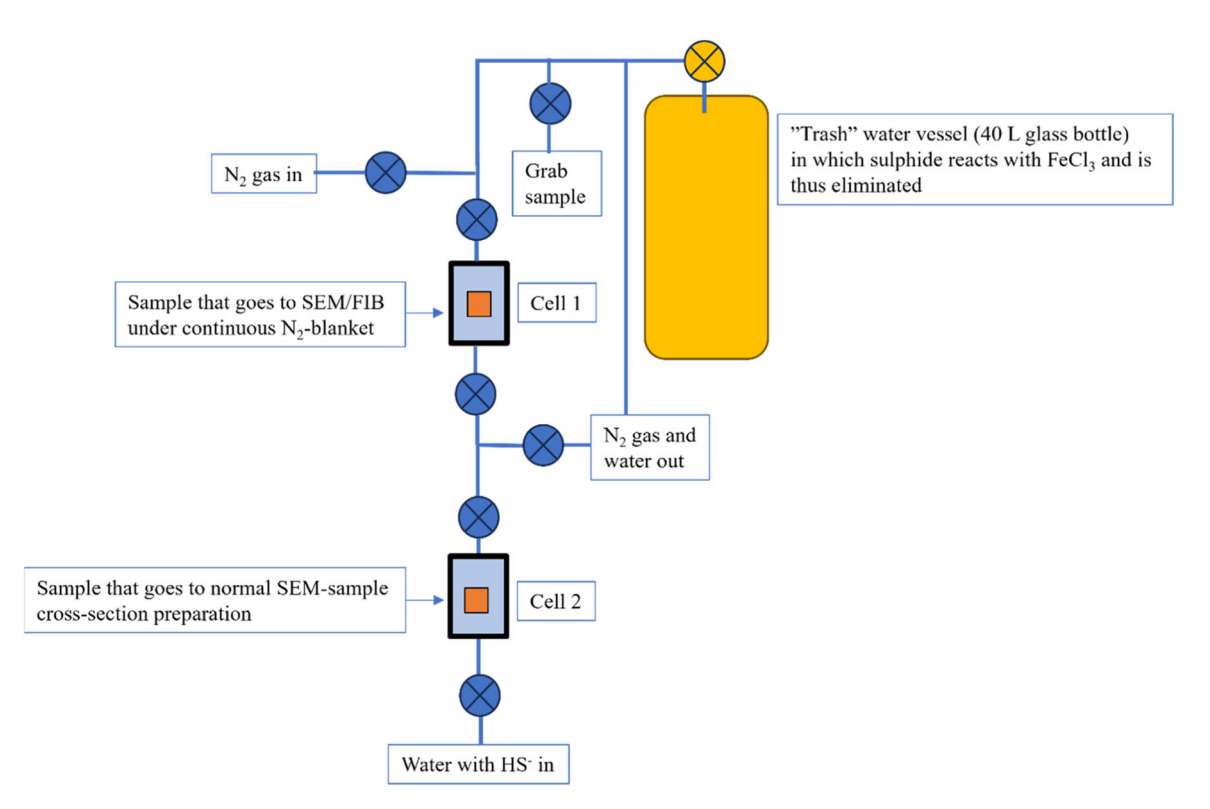


FIGURE 1 | Schematic diagram of the flow through cell arrangement. SEM/FIB, scanning electron microscopy/focused ion beam. [Color figure can be viewed at wileyonlinelibrary.com]

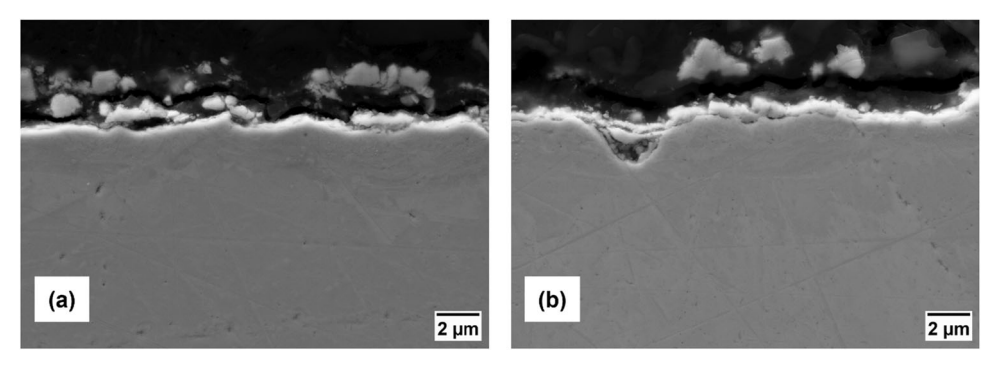


FIGURE 2 | Cross-sectional SEM image of the Cu-OFP sample from Cell 2, (a) Location 1 and (b) location 2. SEM, scanning electron microscopy.

2.4 | SEM and SEM/FIB Characterization

The cross-sectional analysis was performed by secondary electron imaging using a Zeiss Crossbeam 540 field emission SEM with a four-quadrant backscatter detector (FQBD). A TESCAN AMBER X plasma- FIB SEM was used for the FIB analysis. In the FIB-process, first a 30 μ m tungsten (W) bed was deposited on the surface after which an ion beam was used to cut through the tungsten bed and the underlaying surface. Additionally, for both the samples elemental analysis of the surface copper films was performed with energy dispersive X-ray spectroscopy (EDS) at 15 kV and 1.5 nA.

3 | Results

3.1 | SEM and SEM/FIB Characterization

The cross-section sample from Cell 2 was characterized under SEM. SEM images from two locations analyzed are shown in Figure 2a,b. At all the locations, this sample had a rather continuous surface film with a thickness of $0.5-1\,\mu m$. The EDS mapping results performed at Location 1 in Figure 2a is shown in Figure 3. There is a continuous line of O at the Cu-film interface, while the S-containing film on top appears discontinuous. Small traces of both Na and P, presumably from the buffer solution, were also detected.

The sample from Cell 1 showed separate hexagonally shaped crystals on the outer surface, Figure 4a. The surface EDS mapping (Figure 5) of this sample revealed that these crystals are enriched with S and Cu. In addition, Na, P and O from the buffer solution were also detected. Since the sample from Cell 1 was not rinsed, the remnants of the buffer solution dried on the surface during the N₂-gas flow used to vacate the internals of the cell from the sulfide solution, thus explaining the coinciding Na, P, and O residues. In contrast to the cross-sectioned sample from Cell 2, the EDS maps of FIB milling through the surface of this sample, Figure 6, do not show a continuous line of O at the

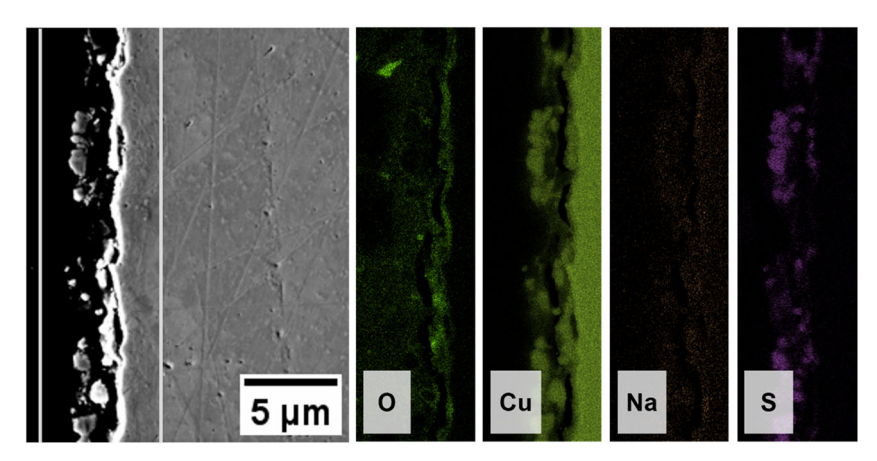


FIGURE 3 | EDS mapping of the cross-sectional sample at Location 1 from Cell 2. EDS, energy dispersive X-ray spectroscopy. [Color figure can be viewed at wileyonlinelibrary.com]

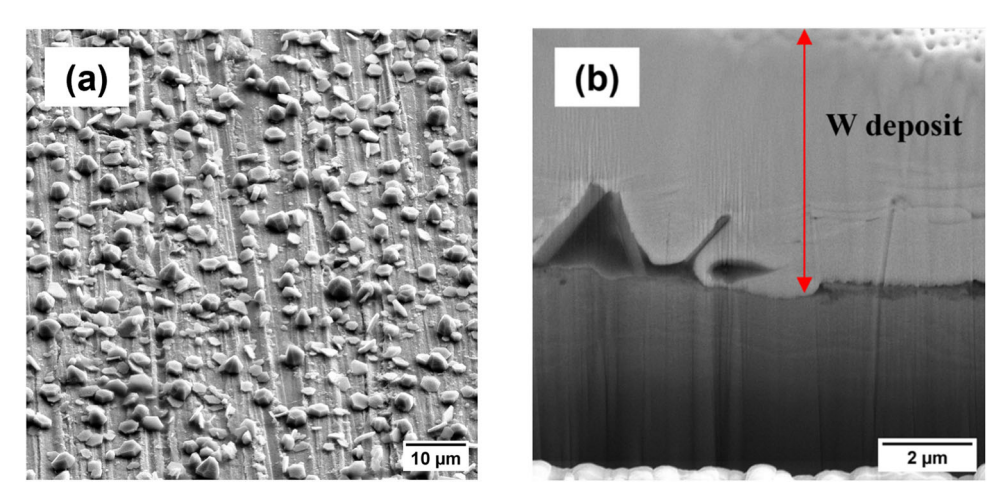


FIGURE 4 | (a) SEM image of the surface of the Cu-OFP sample from Cell 1, (b) cross-sectional image after FIB milling. FIB, focused ion beam; SEM, scanning electron microscopy. [Color figure can be viewed at wileyonlinelibrary.com]

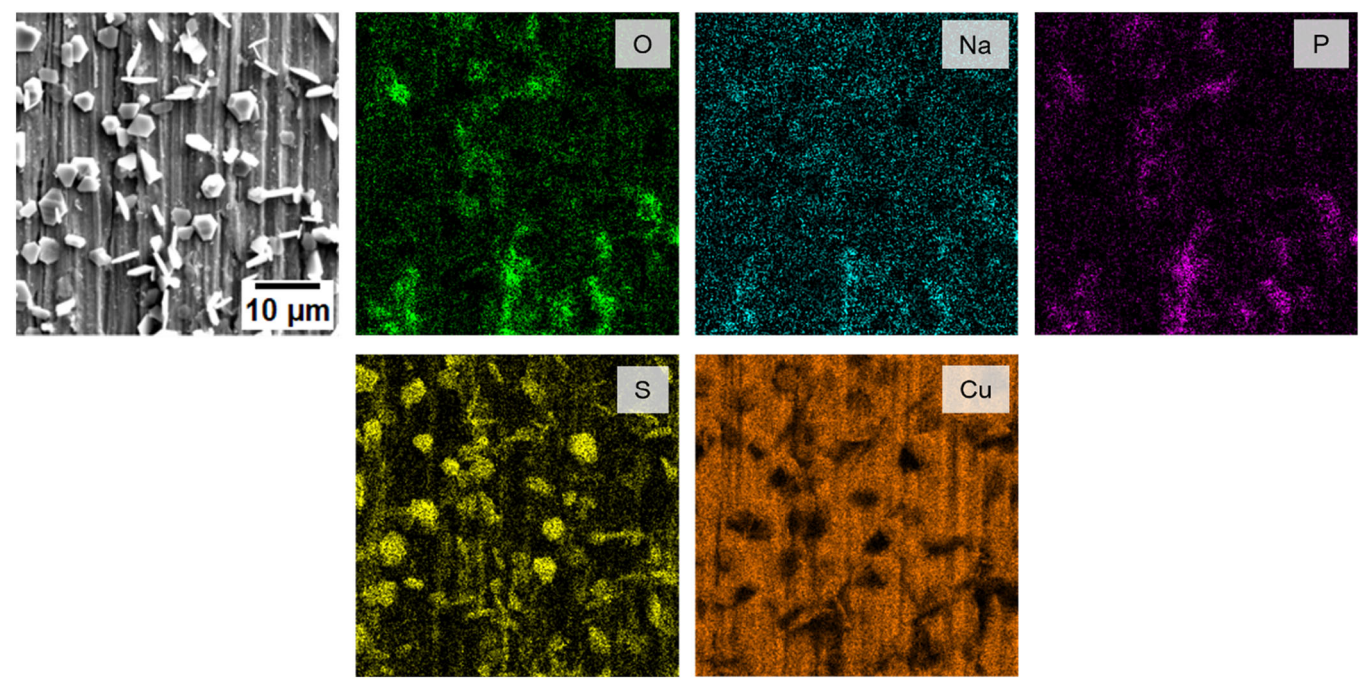


FIGURE 5 | EDS map of the surface of the Cu-OFP sample from Cell 1. EDS, energy dispersive X-ray spectroscopy. [Color figure can be viewed at wileyonlinelibrary.com]

4 Materials and Corrosion, 2025

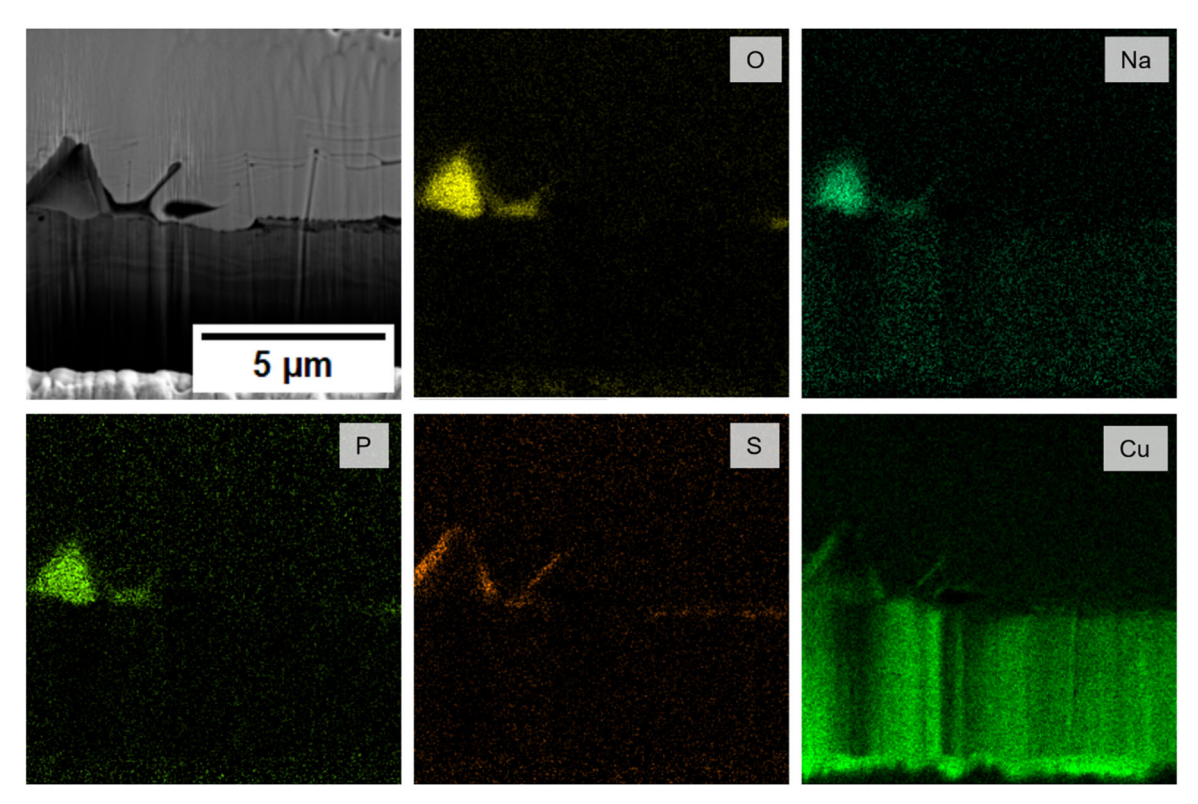


FIGURE 6 | EDS map of the interface after FIB milling of the Cu-OFP from Cell 1. EDS, energy dispersive X-ray spectroscopy; FIB, focused ion beam. [Color figure can be viewed at wileyonlinelibrary.com]

Cu-film interface. Some particles on the surface seem to consist of Na, P, and O, in line with the EDS maps of the outer surface shown in Figure 5. The S and Cu rich surface layer appears discontinuous and nonuniform, suggesting incomplete sulfide nucleation and film growth at the studied concentration, as has been observed previously [19].

3.2 | Linear Polarization Resistance (LPR)

The corrosion potential was measured continuously during the test up until the switch of the buffer source, showing a potential of about $E=-0.65~\rm V_{\rm SHE}$. After the switching of the flow feed to buffer without sulfide, the corrosion potential showed a slow increase reflecting the decrease of sulfide concentration. The LPR plots obtained at varying sulfide concentrations are shown in Figure 7a.

All the cathodic branch curves appeared linear with no major distinctive changes, while a pronounced effect was observed in the anodic branch of the polarization resistance curve for different sulfide concentrations. The current density at the anodic potential of $+30\,\mathrm{mV}$ versus the open circuit potential (OCP) decreased from about $0.098\,\mathrm{mA/cm^2}$ for $30\,\mathrm{mg/L}$ of sulfide to about $0.01\,\mathrm{mA/cm^2}$ when the sulfide concentration dropped to $2\,\mathrm{mg/L}$. Current densities extracted from the LPR plots were plotted as a function of varying sulfide concentrations. The plot in Figure 7b illustrates the relationship between current density and sulfide concentration, revealing a clear increasing trend. A linear model was applied to this data, resulting in the equation y = 0.00539x + 0.01027, where 'y' represents the current density $(\mathrm{mA/cm^2})$ and 'x' denotes the sulfide concentration $(\mathrm{mg/L})$.

The high coefficient of determination $R^2 = 0.99348$ indicates an excellent fit, suggesting that the linear model accurately describes the observed data. This strong correlation underscores the direct proportionality between sulfide concentration in the buffer solution and the measured current density. Therefore, measuring the anodic current density of the Cu-OFP in sulfide containing solution could provide convenient on-line monitoring for the sulfide concentration detection in the water phase. Note that the current density corresponding to the sulfide concentration of 30 mg/L does not follow the linear trend.

4 | Discussion

On comparing the microstructural characterization results of the cross-section sample from Cell 2 and the SEM/FIB cut sample from Cell 1, it clearly shows that in anoxic sulfide solutions there is no formation and presence of an oxide film at the Cu-Cu₂S interface. The oxide film detected in the EDS maps for the cross-sectional sample from Cell 2 in Figure 3 appears to be formed during the sample preparation stage, which involves the use of aerated water. It is important to note that the sample from Cell 2 was cross-sectionally cut before the SEM analysis, whereas the sample from Cell 1 was not. The surface of the latter was cross-sectioned using FIB milling, and any oxide that may form due to brief ambient exposure during the transfer of the coupon to the SEM/FIB chamber from the Cell 1 would likely be too thin to be detected with SEM. Furthermore, even if one argues that there could be a possibility for the flow-through cell system to have experienced some oxygen ingress, the formation of an oxide film would have also occurred on the samples exposed to the sulfide buffer solution in Cell 1.

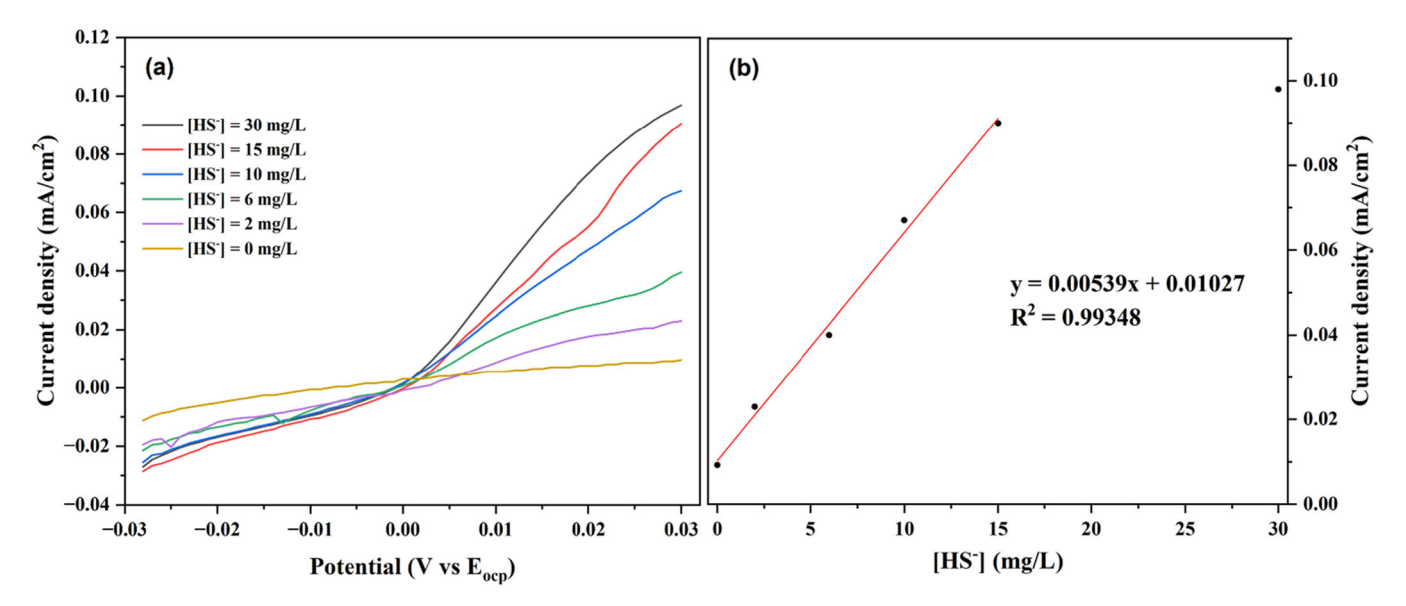


FIGURE 7 | (a) LPR plot of Cu-OFP obtained at varying sulfide concentration. (b) Current density vs sulfide concentration in the buffer solution with a linear fit. LPR, linear polarization resistance. [Color figure can be viewed at wileyonlinelibrary.com]

Therefore, it is unlikely that oxide formation occurs during the 48-h sulfide exposure test. Moreover, any pre-existing copper oxide on the Cu-OFP surface could be expected to convert to Cu₂S when exposed to the sulfide solution by direct chemical reaction between the oxide and HS⁻. Consequently, the surface of Cu-OFP is expected to only consists of the sulfide layer [20], as confirmed by the microscopy results presented in Figure 4.

The surface of the sample from Cell 1 had hexagonally shaped sulfide crystals, Figure 4. These could be expected to be chalcocite (Cu_2S) as the EDS mapping of these crystals revealed them to be rich in S and Cu (Figure 5), similar to what has been reported in [7, 21]. The nucleation and growth of chalcocite crystals is governed dominantly by immersion time in the sulfide solution, eventually covering the surface [7]. Given that the copper samples were exposed in sulfide solution for only 48 h, the copper surface is sparsely covered by chalcocite crystals, which have not fully grown to form a complete sulfide film layer.

The LPR results have shown that the anodic current density exhibits a linearly increasing trend with the sulfide concentration in the buffer solution. This rise in anodic current densities at higher sulfide concentration is caused by the increase in sulfide diffusion flux (mass transfer), which results in surplus availability of sulfide at the copper surface for active corrosion, where the nucleation and formation of the sulfide film (Cu₂S) initiates [7, 15, 22]. Incorporating this copper anodic current density data achieved at various sulfide concentrations in mode of an on-line sensor one can feasibly gain reliable semi-quantitative information regarding the sulfide concentration in the solution at the copper surface with minimal disturbance to the studied system. Additionally, it was noted that in Figure 7b the anodic current density corresponding to the 30 mg/L HS⁻ does not follow the linear trend of the plot. Although not specifically analyzed in this study, the anodic current density at increasing sulfide concentration > 15 mg/L in Figure 7b plateaus consistently between measurements. At sufficiently high HS concentrations (≥ 10^{-3} M), the anodic current becomes almost independent of transport flux and decreases with increasing potential due to some passivation of the Cu surface resulting from the formation of a compact corrosion film [23, 24]. When sulfide depletion was initiated by switching the flow to buffer without sulfur, there might still have been excess HS⁻ at the Cu surface and consequently the Cu surface being covered by a compact sulfide film layer, causing the anodic current density limit to be reached. With a decreasing sulfide concentration leading to a linear anodic current density response, this tends to suggest a fast reorganization or dissolution of the sulfide film, transitioning from a compact film independent of transport flux to a more porous film with transport limitation. The mechanism for such a transition is subject to further study.

5 | Conclusion

The existence and formation of copper oxide at the Cu–Cu₂S interface was investigated in anoxic sulfide bearing phosphate buffer solution in a flow-through cell set up. Post exposure SEM and FIB characterization studies revealed:

- 1. The SEM/EDS results showed that after 48 h exposure, the surface of the copper is sparsely covered with hexagonally shaped chalcocite crystals.
- 2. FIB characterization revealed no presence of oxide on the sample surface which was exposed to an anoxic sulfide solution for 48 h and stored under N_2 blanket.
- 3. The cross-section samples which were immediately removed after 48 h exposure under anoxic sulfide solution showed a presence of oxide on the surface. The metallographic preparation phase during which water is utilized causes oxide formation on the copper sample surface.

Additionally, the presence of 10^{-3} M sulfide in the solution was found to influence the anodic current densities determined

6 Materials and Corrosion, 2025

from the LPR of copper. These anodic current densities were found to linearly decrease with the depleting sulfide content and a linear model equation has been presented, demonstrating the method for measuring sulfide concentration in solution.

Acknowledgments

This study on creep testing in sulfide solutions 233284 was funded by SKB, the Swedish Nuclear Fuel and Waste Management Co. (Solna, Sweden).

Conflicts of Interest

The authors declare no conflicts of interest.

Data Availability Statement

The data that support the findings of this study are available from the corresponding author upon reasonable request.

References

- 1. F. King, C. Lilja, and M. Vähänen, "Progress in the Understanding of the Long-Term Corrosion Behaviour of Copper Canisters," *Journal of Nuclear Materials* 438 (2013): 228–237, https://doi.org/10.1016/j.jnucmat.2013.02.080.
- 2. P. Koho, F. King, T. Prihti, T. Salonen, L. Koskinen, and B. Pastina, "Treatment of Canister Corrosion in Posiva's Safety Case for the Operating Licence Application," *Materials and Corrosion* 74 (2023): 1567–1579, https://doi.org/10.1002/maco.202313778.
- 3. H. C. M. Andersson-Östling, J. Hagström, and M. Danielsson, "SKB R-17-19, Phosphorus in Copper Intended for Spent Nuclear Fuel Disposal," Svensk Kärnbränslehantering AB, 2018.
- 4. J. Chen, Z. Qin, and D. W. Shoesmith, "Long-Term Corrosion of Copper in a Dilute Anaerobic Sulfide Solution," *Electrochimica Acta* 56 (2011): 7854–7861, https://doi.org/10.1016/j.electacta.2011.04.086.
- 5. N. A. Senior, T. Martino, J. Binns, and P. Keech, "The Anoxic Corrosion Behaviour of Copper in the Presence of Chloride and Sulphide," *Materials and Corrosion* 72 (2021): 282–292, https://doi.org/10.1002/maco.202011783.
- 6. M. Bojinov, T. Ikäläinen, Z. Que, and T. Saario, "Effect of Sulfide on De-Passivation and Re-Passivation of Copper in Borate Buffer Solution," *Corrosion Science* 218 (2023): 111201, https://doi.org/10.1016/j.corsci. 2023.111201.
- 7. J. Chen, Z. Qin, and D. W. Shoesmith, "Kinetics of Corrosion Film Growth on Copper in Neutral Chloride Solutions Containing Small Concentrations of Sulfide," *Journal of the Electrochemical Society* 157 (2010): C338, https://doi.org/10.1149/1.3478570.
- 8. T. Martino, J. Chen, Z. Qin, and D. W. Shoesmith, "The Kinetics of Film Growth and Their Influence on the Susceptibility to Pitting of Copper in Aqueous Sulphide Solutions," *Corrosion Engineering, Science and Technology* 52 (2017): 61–64, https://doi.org/10.1080/1478422X. 2017.1297575.
- 9. C. Taxén, A. Moya Núñez, and C. Lilja, "Stress Corrosion of Copper in Sulfide Solutions: Variations in pH-Buffer, Strain Rate, and Temperature," *Materials and Corrosion* 74 (2023): 1632–1644, https://doi.org/10.1002/maco.202313759.
- 10. X. Yue, P. Malmberg, E. Isotahdon, et al., "Penetration of Corrosive Species Into Copper Exposed to Simulated O₂-Free Groundwater By Time-of-Flight Secondary Ion Mass Spectrometry (ToF-SIMS)," *Corrosion Science* 210 (2023): 110833, https://doi.org/10.1016/j.corsci.2022.110833.
- 11. M. Guo, J. Chen, C. Lilja, et al., "The Anodic Formation of Sulfide and Oxide Films on Copper in Borate-Buffered Aqueous Chloride

- Solutions Containing Sulfide," *Electrochimica Acta* 362 (2020): 137087, https://doi.org/10.1016/j.electacta.2020.137087.
- 12. J. M. Smith, J. C. Wren, M. Odziemkowski, and D. W. Shoesmith, "The Electrochemical Response of Preoxidized Copper in Aqueous Sulfide Solutions," *Journal of the Electrochemical Society* 154 (2007): C431, https://doi.org/10.1149/1.2745647.
- 13. V. Ratia-Hanby, E. Isotahdon, X. Yue, et al., "Characterization of Surface Films That Develop on Pre-Oxidized Copper in Anoxic Simulated Groundwater With Sulphide," *Colloids and Surfaces, A: Physicochemical and Engineering Aspects* 676 (2023): 132214, https://doi.org/10.1016/j.colsurfa.2023.132214.
- 14. J. Chen, X. Pan, T. Martino, et al., "The Effects of Chloride and Sulphate on the Growth of Sulphide Films on Copper in Anoxic Sulphide Solutions," *Materials and Corrosion* 74 (2023): 1665–1676, https://doi.org/10.1002/maco.202313766.
- 15. J. Chen, Z. Qin, L. Wu, J. J. Noël, and D. W. Shoesmith, "The Influence of Sulphide Transport on the Growth and Properties of Copper Sulphide Films on Copper," *Corrosion Science* 87 (2014): 233–238, https://doi.org/10.1016/j.corsci.2014.06.027.
- 16. T. Kosec, M. Hren, and A. Legat, "Monitoring Copper Corrosion In Bentonite by Means of a Coupled Multi-Electrode Array," *Corrosion Engineering, Science and Technology* 52 (2017): 70–77, https://doi.org/10.1080/1478422X.2017.1312200.
- 17. T. Välimäki, "SKB T58 Tube Structure Evaluation, SKBdoc 1216615," Luvata Pori Oy, 2009.
- 18. Standard Specification for Reagent Water, "ASTM D1193-24, ASTM International," 2024, https://doi.org/10.1520/D1193-24.
- 19. J. Chen, X. Pan, H. Y. Nie, et al., "Topographical and Statistical Studies of the Corrosion Damage Underneath a Sulfide Film Formed on a Cu Surface," *Corrosion Science* 248 (2025): 112801, https://doi.org/10.1016/j.corsci.2025.112801.
- 20. E. Salehi Alaei, M. Guo, J. Chen, et al., "The Transition From Used Fuel Container Corrosion under Oxic Conditions to Corrosion in an Anoxic Environment," *Materials and Corrosion* 74 (2023): 1690–1706, https://doi.org/10.1002/maco.202313757.
- 21. J. Chen, Z. Qin, T. Martino, and D. W. Shoesmith, "Non-Uniform Film Growth and Micro/Macro-Galvanic Corrosion of Copper in Aqueous Sulphide Solutions Containing Chloride," *Corrosion Science* 114 (2017): 72–78, https://doi.org/10.1016/j.corsci.2016.10.024.
- 22. J. Chen, Z. Qin, and D. W. Shoesmith, "Key Parameters Determining Structure and Properties of Sulphide Films Formed on Copper Corroding in Anoxic Sulphide Solutions," *Corrosion Engineering, Science and Technology* 49 (2014): 415–419, https://doi.org/10.1179/1743278214Y.0000000188.
- 23. T. Martino, J. Smith, J. Chen, Z. Qin, J. J. Noël, and D. W. Shoesmith, "The Properties of Electrochemically-Grown Copper Sulfide Films," *Journal of the Electrochemical Society* 166 (2019): C9–C18, https://doi.org/10.1149/2.0321902jes.
- 24. T. Martino, R. Partovi-Nia, J. Chen, Z. Qin, and D. W. Shoesmith, "Mechanisms of Film Growth on Copper in Aqueous Solutions Containing Sulphide and Chloride Under Voltammetric Conditions," *Electrochimica Acta* 127 (2014): 439–447, https://doi.org/10.1016/j.electacta.2014.02.050.